Available online at www.sciencedirect.com
SCIENCE DIRECT®
ELSEVIER
European Journal of Mechanics B/Fluids 22 (2003) 529–543
EUROPEAN JOURNAL OF MECHANICS B/FLUIDS

Mixed convection boundary-layer flow over a vertical surface embedded in a porous medium

E.H. Aly, L. Elliott, D.B. Ingham *

Department of Applied Mathematics, University of Leeds, Leeds, LS2 9JT, UK

Received 11 March 2003; accepted 11 July 2003

Abstract

In this paper we have numerically investigated the existence and uniqueness of a vertically flowing fluid passed a model of a thin vertical fin in a saturated porous media. We have assumed the two-dimensional mixed convection from a fin, which is modelled as a fixed, semi-infinite vertical surface, embedded in a fluid-saturated porous media under the boundary-layer approximation. We have taken the temperature, in excess of the constant temperature in the ambient fluid on the fin, to vary as $\bar{x}^{\lambda}$, where $\bar{x}$ is measured from the leading edge of the plate and λ is a fixed constant. The Rayleigh number is assumed to be large so that the boundary-layer approximation may be made and the fluid velocity at the edge of the boundary-layer is assumed to vary as $\bar{x}^{\lambda}$. The problem then depends on two parameters, namely λ and ε, the ratio of the Rayleigh to Péclet numbers. It is found that when $\lambda > 0$ (<0) there are (is) dual (unique) solution(s) when ε is grater than some negative values of ε (which depends on λ). When $\lambda < 0$ there is a range of negative value of ε (which depends on λ) for which dual solutions exist and for both $\lambda > 0$ and $\lambda < 0$ there is a negative value of ε (which depends on λ) for which there is no solution. Finally, solutions for $0 < \varepsilon \ll 1$ and $\varepsilon \gg 1$ have been obtained.

Keywords: Porous media; Boundary-layer; Mixed convection; Dual solutions

1. Introduction

Over the last four decades much work has been performed on the study of mixed convection boundary-layer flows. The analogous problems of mixed convection in porous media have important applications in such fields as geothermal energy extraction, oil reservoir modelling, the analysis of insulating systems, food processing, casting and welding in manufacturing processes, the dispersion of chemical contaminants in different industrial processes and in the environment, etc. Convective flows in porous media are of vital importance to these processes, thereby generating the need for their full understanding. Recent books by Ingham and Pop [1], Nield and Bejan [2] and Pop and Ingham [3] on convection flows in porous media demonstrate that external convective flows have become a classical subject.

The possibility of obtaining similarity solutions for mixed convection boundary-layer flows was first considered by Sparrow et al. [4] who showed that the boundary-layer equations could be reduced to a pair of coupled ordinary differential equations and they obtained some solutions. Furthermore, Cheng [5] investigated the mixed convection adjacent to inclined surfaces embedded in a porous medium using the boundary-layer approximation. Similarity solutions have been obtained for the situation where the free stream velocity and the surface temperature distribution vary according to the same power function of the distance along the surface.

* Corresponding author.
E-mail address: amt6dbi@maths.leeds.ac.uk (D.B. Ingham).

0997-7546/$ – see front matter
doi:10.1016/S0997-7546(03)00059-1

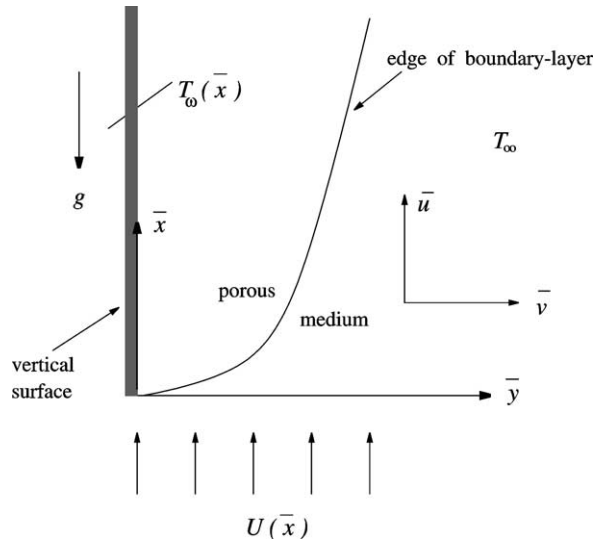

Fig. 1. Schematic diagram of the mathematical model of the problem under investigation and the co-ordinate system employed.

Numerical and asymptotic solutions have been investigated for the boundary-layer equations of mixed convection resulting from the flow over a heated vertical or horizontal flat plate for both aiding, where the flow is directed vertically upwards, and opposing situations, where the flow is directed vertically downwards, i.e., where the buoyancy and inertia forces act in opposite directions. However, the majority of treatments of this problem are limited to the aiding flow case, with the opposing flow case having received much less attention. For the opposing flow the numerical solution breaks down and the boundary-layer may separate from the plate – giving rise to rather unusual heat transfer characteristics. It appears that the separation in mixed convection flow was first discussed by Merkin [6], who examined the effect of opposing buoyancy forces on the boundary-layer flow on a semi-infinite vertical flat plate at a constant temperature in a uniform free stream. Furthermore, this problem was studied by Wilks [7,8] and Hunt and Wilks [9], who also considered the case of uniform flow over a semi-infinite flat plate, but now heated at a constant heat flux rate. Dual solutions of the mixed convection boundary-layer equations for opposing flows on a vertical surface have been studied by Wilks and Bramley [10], Merkin [11], Merkin and Mahmood [12] and Ridha [13]. Merkin and Pop [14] obtained the similarity equations for mixed convection boundary-layer flow over a vertical semi-infinite flat plate in which the free stream velocity is uniform and the wall temperature is inversely proportional to the distance along the plate.

In this paper we have investigated a vertically flowing fluid, in a fluid-saturated porous media which is maintained at a constant temperature, T_∞, past a thin vertical fin, which is modelled as a fixed, semi-infinite vertical surface. The temperature of the fin, above the ambient temperature T_∞, is assumed to vary as $\bar{x}^\lambda$, where $\bar{x}$ is the distance from the tip of the fin and λ is a preassigned constant. The Rayleigh number is assumed to be large so that the boundary-layer approximation may be made and the fluid velocity at the edge of the boundary-layer is assumed to vary as $\bar{x}^\lambda$ so that a similarity solution may be obtained. Fig. 1 schematically illustrates the mathematical model of the problem under investigation.

2. Governing equation

We assume that the convecting fluid and the porous media are isotropic, in thermodynamic equilibrium and have constant physical properties, i.e., the properties of the fluid and the porous media, such as viscosity, thermal conductivity, thermal expansion coefficient, specific heat and permeability, are all constant. The flow is assumed to be described by Darcy's law and we assume that the Boussinesq approximation is valid. On using the following non-dimensional quantities:

$$x = \frac{\bar{x}}{L}, \qquad y = \frac{(Pe)^{1/2}\bar{y}}{L}, \qquad \psi = \frac{\bar{\psi}}{\alpha_m (Pe)^{1/2}}, \qquad \Theta = \frac{\overline{T} - T_\infty}{T_0 - T_\infty}, \tag{1}$$

where $\bar{x}$, $\bar{y}$ are vertical and horizontal co-ordinates, respectively, L is an arbitrary length scale, Pe is the Péclet number $Pe = U_0 L/\alpha_m$, where $U_0 = BL^\lambda$ is the reference velocity, $B > 0$, $\bar{\psi}$ is the stream function, α_m is effective thermal diffusivity of the porous medium and T_0 is the reference temperature, $T_0 = T_\infty + |A|L^\lambda$. Then the governing equations are given by, see Cheng and Minkowycz [15],

$$\frac{1}{Pe}\frac{\partial^2\psi}{\partial x^2}+\frac{\partial^2\psi}{\partial y^2}=\frac{Ra}{Pe}\frac{\partial\Theta}{\partial y}, \tag{2}$$

$$\frac{\partial\psi}{\partial y}\frac{\partial\Theta}{\partial x}-\frac{\partial\psi}{\partial x}\frac{\partial\Theta}{\partial y}=\frac{1}{Pe}\frac{\partial^2\Theta}{\partial x^2}+\frac{\partial^2\Theta}{\partial y^2}, \tag{3}$$

where Ra is the Rayleigh number, $Ra = gK\beta L(T_0 - T_\infty)/(\nu\alpha_m) = gK\beta|A|L^{\lambda+1}/(\nu\alpha_m)$, where g is the magnitude of the acceleration due to gravity, K is the permeability of the porous media, β is the coefficient of thermal expansion and ν is the kinematic viscosity of the fluid.

On assuming that the Péclet number is very large, the resulting temperature boundary-layer is analogous to that in classical boundary-layer theory. Therefore, by letting $Pe \to \infty$ in Eqs. (2) and (3), we obtain the following boundary-layer equations:

$$\frac{\partial^2\psi}{\partial y^2}=\varepsilon\frac{\partial\Theta}{\partial y}, \tag{4}$$

$$\frac{\partial\psi}{\partial y}\frac{\partial\Theta}{\partial x}-\frac{\partial\psi}{\partial x}\frac{\partial\Theta}{\partial y}=\frac{\partial^2\Theta}{\partial y^2}, \tag{5}$$

where the mixed convection parameter ε is defined as

$$\varepsilon=\frac{Ra}{Pe}. \tag{6}$$

Eqs. (4) and (5) have to be solved subject to the boundary conditions that there is no normal velocity on the plate, the temperature of the plate is $T_\infty + A\bar{x}^\lambda$ and the vertical component of the fluid velocity at the edge of the boundary-layer is $B\bar{x}^\lambda$. On using the non-dimensionlisation (1), the boundary conditions become:

$$\psi=0,\quad \Theta=x^\lambda\ (A>0)\quad\text{or}\quad \Theta=-x^\lambda\ (A<0),\quad \text{on } y=0,\ 0<x<\infty, \tag{7}$$

$$\frac{\partial\psi}{\partial y}\to x^\lambda,\quad \Theta\to 0,\quad \text{as } y\to\infty,\quad 0<x<\infty. \tag{8}$$

We seek similarity solutions of Eqs. (4) and (5), subject to the boundary conditions (7) and (8) by introducing the dimensionless similarity variables:

$$\psi(x,y)=\left(2x^{\lambda+1}\right)^{1/2}f(x,\eta),\quad \eta=\frac{y}{(2x^{1-\lambda})^{1/2}},\qquad \Theta(x,y)=x^\lambda\theta(x,\eta), \tag{9}$$

where f is a function to be determined. Hence, we obtain

$$f'=1+\varepsilon\theta, \tag{10}$$

$$\theta''+(1+\lambda)f\theta'-2\lambda f'\theta=0, \tag{11}$$

which have to be solved subject to the boundary conditions:

$$f=0,\quad \theta=1\ (A>0)\quad\text{or } \theta=-1\ (A<0),\quad \text{on } \eta=0, \tag{12}$$

$$f'\to 1,\quad \theta\to 0,\quad \text{as } \eta\to\infty. \tag{13}$$

In order to simplify the mathematical formulation when $A<0$, namely when $\theta(x,0)=-1$, θ is replaced by $(-\theta)$ and the negative sign in Eq. (10) is incorporated into the parameter ε. Hence, regardless of whether the vertical surface is heated or cooled, Eqs. (10) and (11) remain the same, but for the sign of the parameter ε. In addition, the value of $\theta(x,0)$ is now always unity. Eqs. (10) and (11) can be combined to give the following single equation:

$$f'''+(1+\lambda)ff''+2\lambda\left(1-f'\right)f'=0, \tag{14}$$

which has to be solved subject to the boundary conditions

$$f(0)=0,\qquad f'(0)=1+\varepsilon,\qquad f'\to 1,\quad \text{as } \eta\to\infty. \tag{15}$$

Thus we observe that the solution of these equations depends on the two parameters, namely λ, which comes from the surface temperature condition, and ε, which is the ratio of the Rayleigh and Péclet numbers. It should be noted that for an isothermal surface, i.e., $\lambda=0$, Eq. (14) and boundary conditions (15) reduce to a problem which has been studied by Merkin [16]. Further, the forced, aiding mixed and opposing mixed convection arise when $\varepsilon=0$, $\varepsilon>0$ and $\varepsilon<0$, respectively.

A quantity of practical importance in convection problems is the heat transfer through the surface into or out of the fluid, namely

$$\bar{q} = -k\left(\frac{\partial \overline{T}}{\partial \bar{y}}\right)_{\bar{y}=0} = -\frac{k(T_0 - T_\infty)}{L}\left(\frac{x^{3\lambda+1}}{2}\right)^{1/2}(Pe)^{1/2}\frac{f''(0)}{\varepsilon}. \tag{16}$$

We now define the local Nusselt number, Nu_x, to be

$$Nu_x = \frac{\bar{q}}{T_\omega - T_\infty}\frac{L}{k} = \left(\frac{x^{3\lambda+1}}{2}\right)^{1/2}(Pe)^{1/2}\frac{f''(0)}{\varepsilon}. \tag{17}$$

Thus one of the most important features of this problem is to study the variation of $f''(0)$ as a function of the parameters ε and λ. Further, it should be noted that the parameter ε is positive for a heated plate and the resulting flow is called assisting (or aiding), and negative for a cooled plate and the resulting flow is called opposing.

3. Numerical techniques

The NAG routine DO2HBF has been used to solve this problem. In general we have found that, for a given value of λ, there are two solutions for a range of values of ε, namely, there is what we refer to as an upper solution, f_u, corresponding to the largest value of $f''(0)$, and a lower solution, f_l, corresponding to the smallest value of $f''(0)$, with $f_l''(0) < f_u''(0)$. In order to solve the governing ordinary differential equations we have used two techniques. In the first, we fixed the value of ε and obtained the two values of $f''(0)$ over much of the ε space. In the second technique, we fixed the value of $f''(0)$ and obtained the value of ε in order to complete the solution for the remainder of the ε space and to obtain the lower solution when $f_l''(0) \to 0$.

4. Results for various values of λ

There are two configurations to study, namely flows aided and flows opposed by the convection. For $\lambda = 0$, Cheng [5] found in the aiding situation, solutions for all values of ε, while in the opposing situation, solutions only for $-1 \leqslant \varepsilon \leqslant 0$. Furthermore, Merkin [16] studied the mixed convection boundary-layer flow about a vertical flat impermeable surface embedded in a saturated porous medium. Merkin [16] found that the full equations have one solution in the range $-1 \leqslant \varepsilon \leqslant 0$ and no solution for $\varepsilon < \varepsilon_{b_1}(\varepsilon_{b_1} \approx -1.354)$, while for $\varepsilon_{b_1} \leqslant \varepsilon < -1$, there are two solutions. In addition, one of the main aims of this paper is to find the exact value of ε at which the curve of $f_l''(0)$ as a function of ε terminates for $\varepsilon < 0$ when $\lambda \leqslant 0$, since it is only when the fluid is being cooled, i.e., in the opposing case, that such a phenomenon can prevail. Thus in this section we extend the work

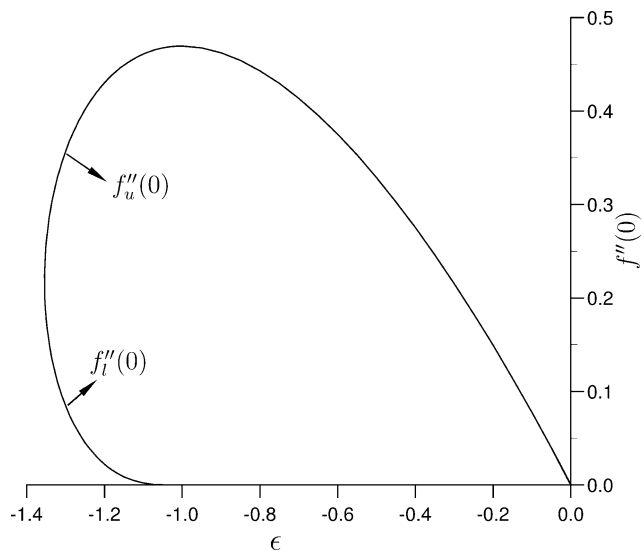

Fig. 2. Variation of $f''(0)$ as a function of ε for $\lambda = 0$ and $\varepsilon \leqslant 0$.

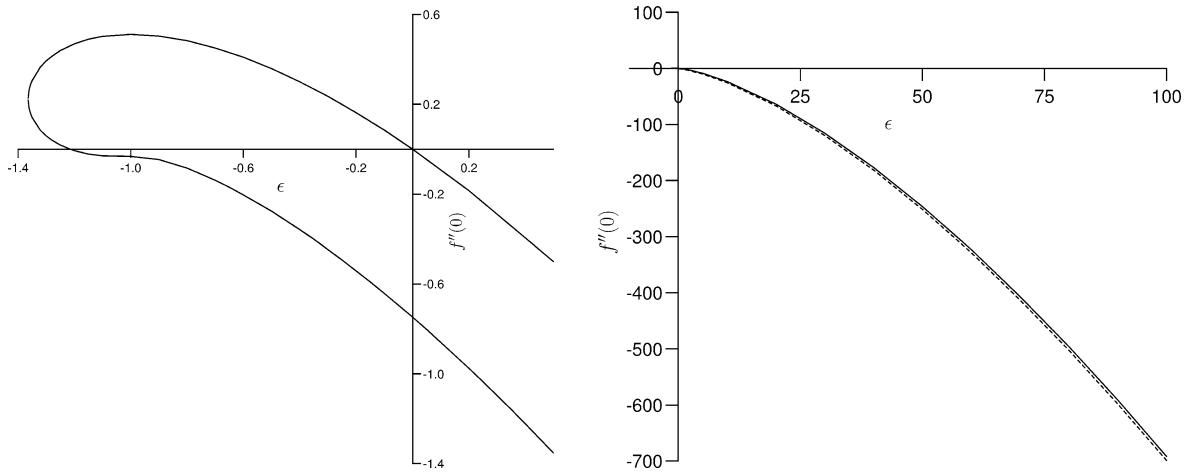

(a) (b)

Fig. 3. Variation of $f''(0)$ as a function of ε for $\lambda = 0.05$ and (a) $-1.364 \leqslant \varepsilon \leqslant 0.5$ and (b) $-1.364 \leqslant \varepsilon \leqslant 100$.

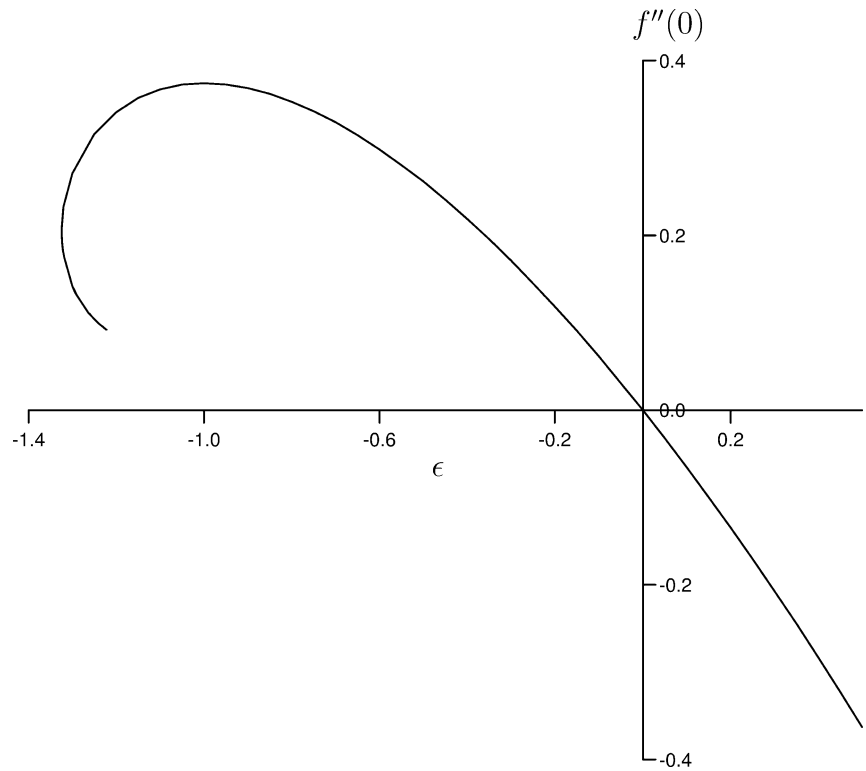

Fig. 4. Variation of $f''(0)$ as a function of ε for $\lambda = -0.1$ and $\varepsilon \leqslant 0.5$.

reported by Merkin [16,11] to investigate further numerical solutions and to produce a more thorough discussion concerning the velocity profiles and shear stress.

We have solved the full equations for $\lambda = 0$ and Fig. 2 shows the variation of $f''(0)$ as a function of ε for $\varepsilon \leqslant 0$. We observe that for $\varepsilon = -1$ the second boundary condition of Eq. (15) equals zero and we have the solution of the Blasius problem with $f_u''(0) = 0.4696$, which is the greatest value of $f''(0)$. Furthermore, there is a range of values of ε, namely $\varepsilon_{b_1} \leqslant \varepsilon < -1$, for which there are two solutions, and as $\varepsilon \to -1^-$ then it appears that $f_l''(0) \to 0$.

For $\lambda > 0$, we have solved the full equations for $\lambda = 0.05$, as an example of the results we have obtained for $\lambda > 0$, since the results for the other values of λ in this range are very similar. We have found that there are two solutions in the range $\varepsilon_{b_2} \leqslant \varepsilon < \infty$ ($\varepsilon_{b_2} = -1.3640$). Fig. 3 shows the variation of $f''(0)$ as a function of ε for $\varepsilon_{b_2} \leqslant \varepsilon \leqslant 0.5$. We observe that the two solutions are negative in the range $0 < \varepsilon < \infty$. However, in the range $\varepsilon_{b_2} < \varepsilon < 0$ the upper solution $f_u''(0)$ is positive while the lower solution $f_l''(0)$ is positive in the range $\varepsilon_{b_2} < \varepsilon < \varepsilon_c$ ($\varepsilon_c \approx -1.2164$ where $f_l''(0) = 0$) and negative in the range $\varepsilon_c < \varepsilon < 0$. Finally, we have evaluated ε_c, ε_{b_2} and $f_l''(0)$ for $\lambda = 0.1,\ 0.2, \ldots$ and 1 and we have found that ε_c and ε_{b_2} decreases, whilst $f_l''(0)$ increases, as λ increases.

For $\lambda < 0$, we have solved the full equations and Fig. 4 shows the variation of $f''(0)$ as a function of ε for $\varepsilon_{b_3} \leqslant \varepsilon \leqslant 0.5$ ($\varepsilon_{b_3} \approx -1.3241$) for $\lambda = -0.1$, which is a representative example of the results we have obtained from all the calculations performed in the range $-1 \leqslant \lambda < 0$ and $\varepsilon_{b_3} \leqslant \varepsilon \leqslant 0.5$. We observe that the curve appears to terminate at ε_t, where $\varepsilon_t \approx -1.2222$, and we were unable to obtain $f''(0)$ for $\varepsilon > \varepsilon_t$. Furthermore, we found that whilst there is a unique solution in the range $\varepsilon_t \leqslant \varepsilon < \infty$, there are two solutions in the range $\varepsilon_{b_3} \leqslant \varepsilon \leqslant \varepsilon_t$. Although $f''(0)$ is negative in the range $\varepsilon > 0$ and increases as ε decreases until $f''(0) = 0$ at $\varepsilon = 0$, $f''(0)$ is positive in the range $\varepsilon < 0$ and increases as ε decreases. In general, we found that the solutions for $\lambda < 0$ are very different from those obtained for $\lambda > 0$, with nearly the same behaviour to those obtained for $\lambda = 0$.

4.1. Velocity profiles

In Fig. 5, for $\lambda = 0$, we observe that the lower solution goes from the left to the right as ε increases and goes rapidly to unity in the outer region of the boundary-layer. Furthermore, if we increase the value of ε, then this solution remains virtually constant over some interval of η, the size of the interval depending on the value of η, before going rapidly to unity. The interval of η over which $f_l'(\eta)$ remains constant increases as the value of ε increases. In addition, it appears that the curves in the outer region of the boundary-layer are virtually identical, with the value of η_∞ that we have to take to represent the location of the outer boundary for the upper solution much smaller than the η_∞ of the lower solution, and the η_∞ of the lower solution changing rapidly as ε increases.

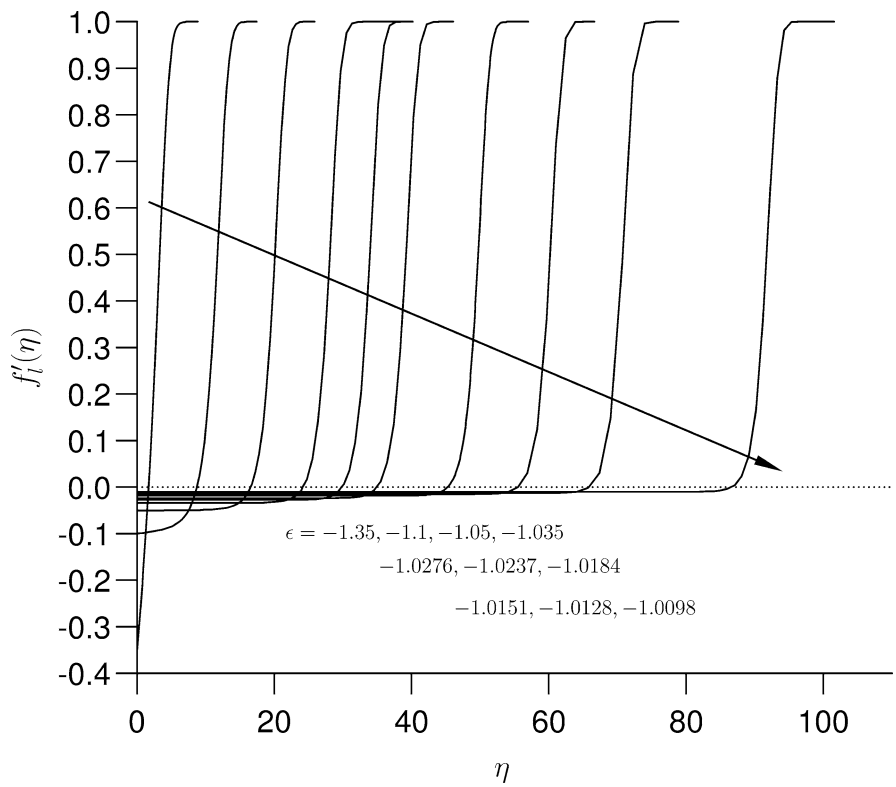

Fig. 5. Profiles of the vertical component of the fluid velocity for $\lambda = 0$ and $\varepsilon = -1.35, -1.1, -1.05, -1.035, -1.0276, -1.0237, -1.0184, -1.0151, -1.0128$ and -1.0098, corresponding to the lower solution.

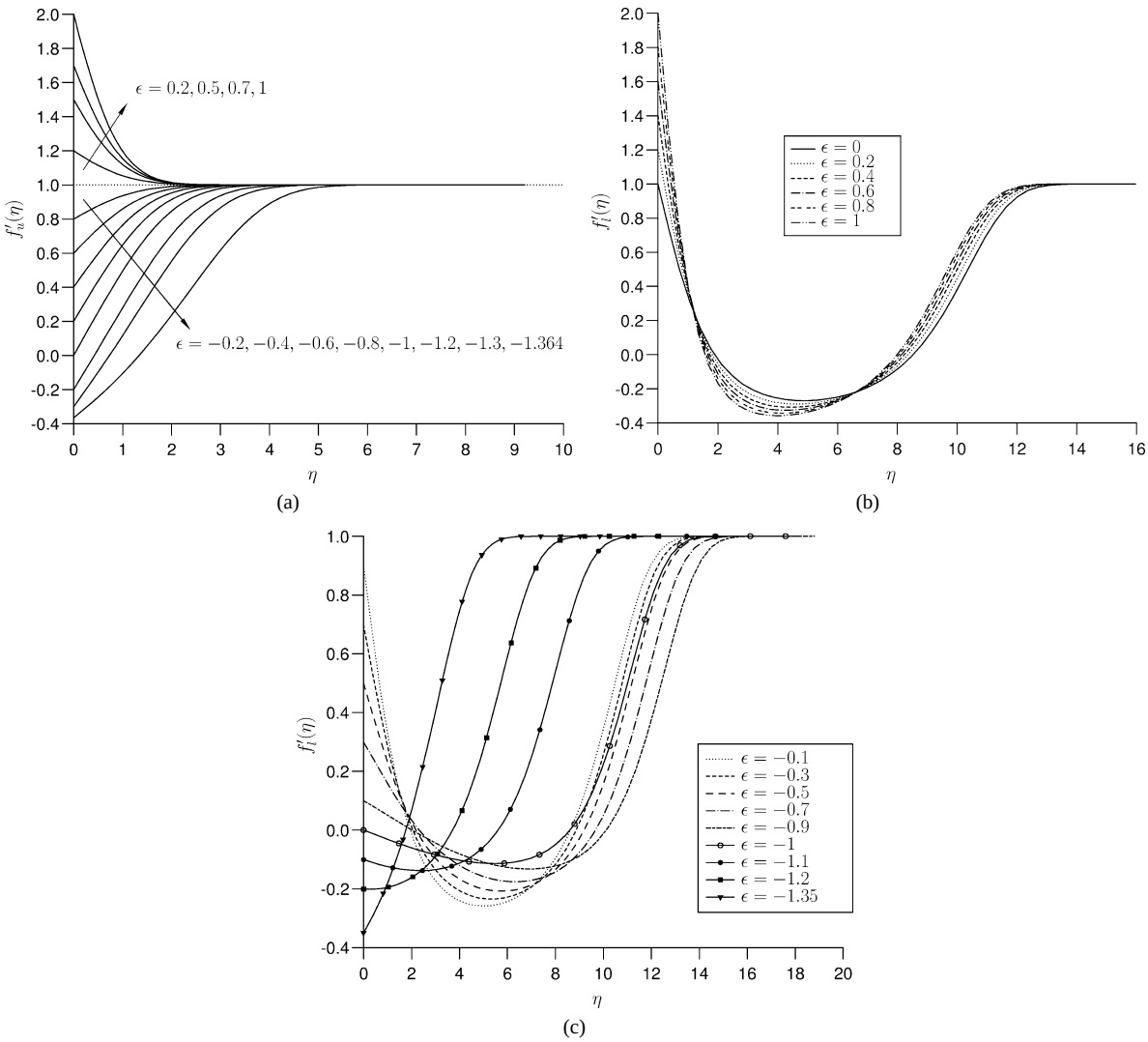

Fig. 6. Profiles of the vertical component of the fluid velocity for $\lambda = 0.05$ and (a) $\varepsilon = 0.2$, 0.5, 0.7, 1 and $\varepsilon = -0.2, -0.4, -0.6, -0.8, -1, -1.2, -1.3, -1.364$, corresponding to the upper solution, (b) $\varepsilon = 0, 0.2, 0.4, 0.6, 0.8$ and 1, corresponding to the lower solution, and (c) $\varepsilon = -0.1, -0.3, -0.5, -0.7, -0.9, -1, -1.1, -1.2$ and -1.35, corresponding to the lower solution.

For $\lambda > 0$, the upper solutions are similar to those for $\lambda = 0$, as shown in Fig. 6(a), whilst the lower solutions are very dependent on the value of ε, as shown in Figs. 6(b) and 6(c). When $\varepsilon > 0$, the lower solutions decrease rapidly from some positive value, cut the η-axis around $\eta \lesssim 1.15$, then have minimum between $1.15 \lesssim \eta \lesssim 6.65$, before returning to a positive value and levelling out at the value of unity. When $-1 < \varepsilon < 0$, the lower solutions behave virtually the same, but the limits of the ranges are different and the boundary-layer thickness is greater, as shown in Fig. 6(c). However, in the range $\varepsilon_{b_2} < \varepsilon < -1$ the lower solutions appear different.

For $\lambda < 0$ and $\varepsilon > 0$, and for $\lambda < 0$ and $\varepsilon_{b_3} \leqslant \varepsilon < 0$, the upper solutions are similar to those obtained by Cheng [5] and Merkin [16,11], respectively, when $\lambda = 0$. Furthermore, for $\lambda < 0$ and $\varepsilon_{b_3} \leqslant \varepsilon < \varepsilon_t$, the lower solutions are similar to the present work when $\lambda = 0$, where ε_t is the largest value of ε for which a lower solution can be found at that particular value of λ.

4.2. Shear stress

From Fig. 7, for $\lambda = 0$, we observe that for ε at the lower end of the range $\varepsilon_{b_3} < \varepsilon < -1$ the shear stress increases rapidly to a maximum before returning rapidly to zero as $\eta \to \eta_\infty$, where η_∞ relatively small. For values of ε near $\varepsilon = -1^-$ the shear

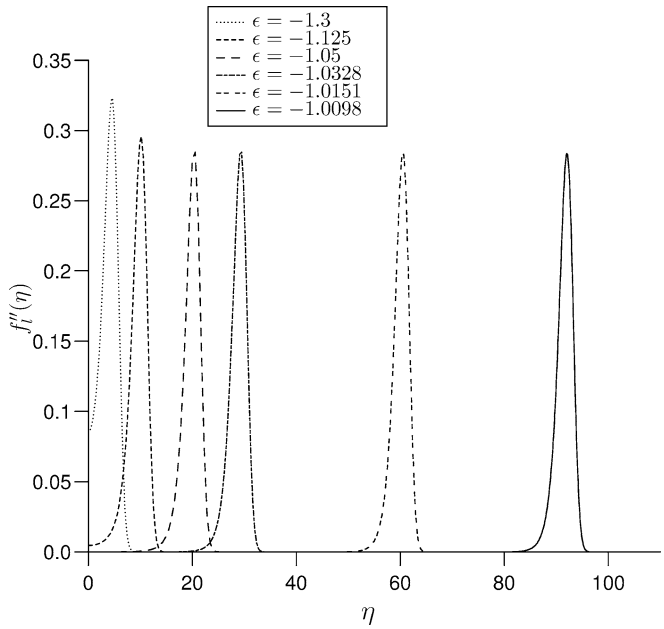

Fig. 7. Variation of the shear stress as a function of η for $\lambda = 0$ and $\varepsilon = -1.3, -1.125, -1.05, -1.0328, -1.0151$ and -1.0098, corresponding to the lower solution.

stress remains virtually zero over some interval of η, the size of the interval depending on the value of ε, then it goes rapidly to a maximum before rapidly returning to zero as $\eta \to \eta_\infty$, where η_∞ is now relatively large.

Figs. 8(a)–(d) are now used to discuss the shear stress in the range $\lambda > 0$. For $\varepsilon > 0$, $f_u''(\eta)$ is negative, with its maximum magnitude at $\eta = 0$, and tends gradually to zero at η_∞. In addition, its magnitude decreases as ε decreases for a fixed value of η. When $-1 \leqslant \varepsilon < 0$, then $f_u''(\eta)$ becomes positive, but again with its maximum magnitude at $\eta = 0$. The shear stress reduces gradually to zero at η_∞, increasing as ε decreases for a fixed value of η. For $\varepsilon_{b_2} \lesssim \varepsilon < -1$, $f_u''(\eta)$ is still positive, but now it increases to a maximum before it gradually decreases to zero, decreasing as ε decreases for a fixed value of η. However, for $f_t''(\eta)$ in this range λ, then when $\varepsilon > 0$ the shear stress increases gradually from a negative value at $\eta = 0$ to zero at η_∞ through four regions, namely from $\eta = 0$ to η_1, where $\eta_1 \approx 2$, from η_1 until η_2, where $f_t''(\eta_2) = 0$, from η_2 to a maximum at $\eta = \eta_3$, where $f_t'''(\eta_3) = 0$, before finally returning to $f_t''(\eta_\infty) = 0$. We observe that the magnitude of the shear stress decreases and increases as ε decreases in the first and fourth regions, respectively. While the magnitude of the shear stress decreases and increases as ε increases in the second and third regions, respectively. Furthermore, in the second region, which is close to $f_t''(\eta) = 0$, then all the curves are very similar. When $-1 \leqslant \varepsilon < 0$, $f_t''(\eta)$ is negative before going to zero at η_∞ through three regions, namely from $\eta = 0$ to η_4, where $\eta_4 \approx 3$, from η_4 to a maximum at $\eta = \eta_5$, where $f_t'''(\eta_5) = 0$, before finally returning to $f_t''(\eta_\infty) = 0$. We observe that in the first region the shear stress is almost linear near the wall, with its gradient increasing as ε decreases. When $\varepsilon_{b_2} \lesssim \varepsilon \leqslant -1$, $f_t''(\eta)$ increases to the maximum before decreasing to zero at η_∞, where the maximum value increases as ε decreases.

For $\lambda < 0$ and $\varepsilon > 0$, and for $\lambda < 0$ and $\varepsilon_{b_3} \leqslant \varepsilon < 0$, the upper solutions are similar to those obtained by Cheng [5] and Merkin [16,11], respectively, when $\lambda = 0$. Furthermore, for $\lambda < 0$ and $\varepsilon_{b_3} \leqslant \varepsilon < \varepsilon_t$, the lower solutions are similar to the present work when $\lambda = 0$.

4.3. Universal curve

From Fig. 5, we observe that the velocity profiles, $f_t'(\eta)$, in the outer region of the boundary-layer are very similar in shape for all values of ε close to -1. They are simply translated a certain distance in the η direction and this translated distance increases with decreasing values of ε. Furthermore, we observe that, for values of ε close to -1, these velocity profiles are similar in shape, but again translated in the η direction, with the solution at $\varepsilon = -1$ on the upper curve. Therefore we postulate that the solutions on the lower curve for large values of η and ε close to -1 are self similar to the solution obtained for $\varepsilon = -1$ on the upper curve, i.e., they follow a universal curve in shape but not in location. Thus in this subsection we investigate the similarity between the upper and the lower solutions for some values of ε near $\varepsilon = -1^-$ and also between the lower solutions

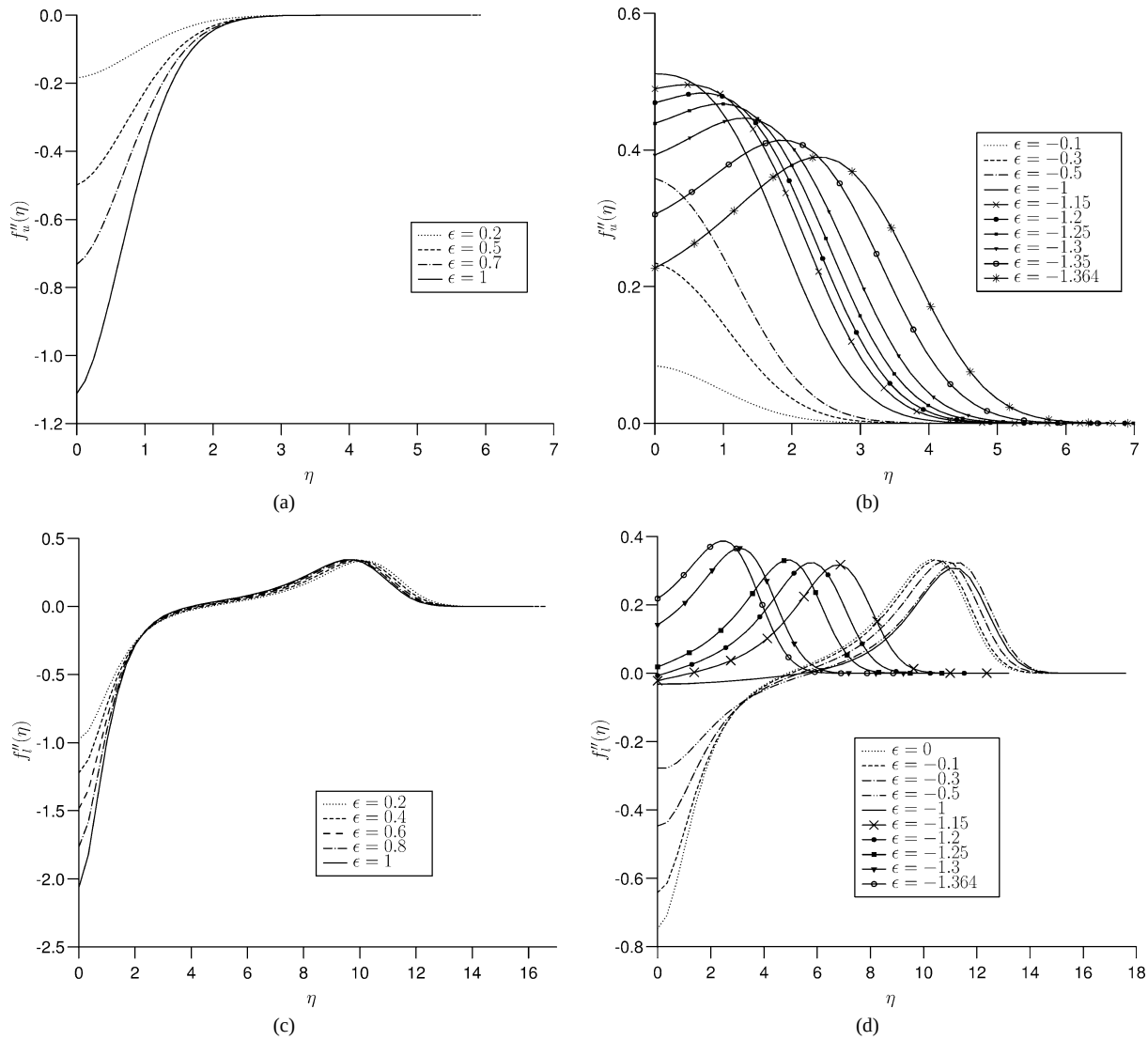

Fig. 8. Variation of the shear stress as a function of η for $\lambda = 0.05$ and (a) $\varepsilon = 0.2, 0.5, 0.7$ and 1, corresponding to the upper solution, (b) $\varepsilon = -0.1, -0.3, -0.5, -1, -1.15, -1.2, -1.25, -1.3, -1.35$ and -1.364, corresponding to the upper solution, (c) $\varepsilon = 0.2, 0.4, 0.6, 0.8$ and 1, corresponding to the lower solution, and (d) $\varepsilon = 0, -0.1, -0.3, -0.5, -1, -1.15, -1.2, -1.25, -1.3$ and -1.364, corresponding to the lower solution.

for some values of ε and the lower solution when $\varepsilon_t = \varepsilon_0$, where ε_0 is the largest value of ε for which the numerical solution $f_t''(\eta)$ can be obtained when $\lambda = 0$.

We have translated the vertical component of the velocity from the upper solution onto the vertical component of the velocity corresponding to the lower solution, for $\varepsilon = -1.05, -1.04, -1.037$ and ε_0. This movement of the upper solution to the lower solution as the gradient of the lower solution on the vertical surface tends to zero has indicated only a slight similarity between the upper and lower solutions when $\varepsilon \to -1^-$. Furthermore, we have translated the vertical component of the velocity from the lower solution when $\varepsilon = -1.05, -1.075, -1.1$ and -1.125 to the vertical component of the velocity corresponding to the lower solution at $\varepsilon = \varepsilon_0$. This movement of the lower solutions for these values to the lower solution for $\varepsilon = \varepsilon_0$ has been undertaken in order to see whether there is any similarity between these lower solutions and the lower solution for $\varepsilon = \varepsilon_0$ when $\varepsilon_0 \to -1^-$ and we have found strong similarity for the region $f'(\eta) \geqslant 0$.

However, it is still unclear whether the solution in the outer part of the boundary-layer establishes a universal curve as $\varepsilon_0 \to -1^-$ for which the velocity profile $f_t''(0) \to 0$. A result that seemed likely when observing the lower solution in Fig. 5 above the value of η for which $f_t'(\eta)$ remains constant over a considerable interval. The question of a possible universal curve

is now approached from a slightly different aspect than simply translating the origin of η by a Transfer Distance, TD, for each lower solution until $f_l'(\eta_2(\varepsilon)) = f_l'(\eta_2(\varepsilon_0)) = 0.5$ and $\eta_2(\varepsilon) + \mathrm{TD} = \eta_2(\varepsilon_0)$. Since, regardless of the value of $f_l'(\eta)$ at which the curves are equated, the exact limiting curve $f_l'(\eta)$ at $\varepsilon = -1$ is not available. Hence, on the basis that for each value of ε there is a TD by which the lower solution can be moved to the lower solution at $\varepsilon = \varepsilon_0$, the solutions are matched at $f_l'(\eta) \to 0$, and the limiting situation studied.

From Fig. 5, we observe that the curve cuts the η-axis at a point near η_∞ so we have studied the relation between f_l' and f_l'' at η_0, where $f(\eta_0) = 0$, in order to investigate the possibility of replacing the boundary condition at the wall by another suitable condition which is independent of the value of ε. We have found that $f_l''(\eta_0)/f_l'(\eta_0) \approx 0.5$ as $\varepsilon \to -1^-$. Hence, if a universal curve exists for the outer region of the boundary-layer as $\varepsilon \to -1^-$, then this curve can be determined by solving the ordinary differential equation

$$f_l''' + f_l f_l'' = 0, \tag{18}$$

subject to the boundary conditions

$$f_l(0) = 0, \qquad f_l''(0) = 0.5 f_l'(0), \qquad f_l' \to 1, \quad \text{as } \eta \to \infty. \tag{19}$$

We have translated the vertical component of the velocity corresponding to the lower solution, which has been obtained from Eq. (18) and the boundary conditions (19), to the vertical component of the velocity corresponding to the lower solution from the full equations when $\varepsilon = -1.113, -1.063, -1.043$ and ε_0. We have found that $f_l'(\eta)$ is virtually the same at these values of ε.

For $\lambda < 0$, we found that the solutions behaved similar to the case when $\lambda = 0$ and therefore we repeated all the steps which we had performed hitherto for $\lambda = 0$, we obtained similar results. Moreover, approaching the chosen points of transfer, when we transferred the lower solutions, $f_l'(\eta)$, for $\lambda = -0.1$ to the lower solutions for $\lambda = 0$, we found that the results virtually coincided above $f'(\eta) = 0.5$, suggesting the possibility of a universal curve which is independent of λ.

4.4. Inner solution

Merkin [16,11] investigated the solution in the vicinity of $\varepsilon = -1$ and found numerically that as $\varepsilon \to -1^-$ then $f_l''(0) \to 0$. Therefore he postulated that the variation of $f''(0)$ with ε terminated at $\varepsilon = -1$ and established a theory accordingly. Furthermore, in the inner region he found that $f_l \simeq (1+\varepsilon)\eta$ but, in the present work, we have established this result analytically using his assumptions as follows: on using the following transformation

$$f_l(\eta) = (1+\varepsilon) F_l(\eta), \tag{20}$$

then Eq. (14), near $\varepsilon = -1$, and the boundary conditions (15) become

$$F_l''' + 2\lambda F_l' = 0, \tag{21}$$

$$F_l(0) = 0, \qquad F_l'(0) = 1, \qquad F_l' \to \infty, \quad \text{as } \eta \to \infty. \tag{22}$$

On integrating Eq. (21) once, and using the first boundary condition in (22), we obtain

$$F_l'' + 2\lambda F_l = F_l''(0), \tag{23}$$

which has to be solved subject to the other boundary conditions in (22). On solving equation (23) for $\lambda = 0$, using the boundary condition (22) twice, and then substituting into equation (20), as $f_l''(0) \to 0$, we obtain

$$f_l(\eta) = (1+\varepsilon)\eta. \tag{24}$$

We now investigate the work of Merkin [11], who used the transformation $\varepsilon = -1 - \alpha$ where $\alpha \geqslant 0$, and found that as $\alpha \to 0^+$ then

$$f_l''(0) = A_1 \mathrm{e}^{-a_0^2/2\alpha} + \cdots, \tag{25}$$

where A_1 is an unknown constant and a_0 is a constant to be determined. Hence the value of $f_l''(0)$ can be found for any value of α, thus avoiding the difficulty of obtaining $f_l''(0)$ numerically. Merkin [11] used the value of a_0 that was determined numerically by Chapman [17], namely $a_0 = 0.8758$, and calculated the quantity

$$Q = f_l''(0)\, \mathrm{e}^{a_0^2/2\alpha}, \tag{26}$$

which should approach the constant value A_1 as $\alpha \to 0$. From Table 1, we observe that we were able to obtain solutions for values of α much closer to 0^+ than those obtained by Merkin [16,11], who initially found $A_1 \approx 0.087$ and then updated it

Table 1
Variation of $f_\iota''(0)$ as a function of α for values approaching $\alpha = 0$ and their corresponding values of Q, as obtained by Merkin [11] and by the present work

	Merkin [11]		Present	
α	$f_\iota''(0)$	Q	$f_\iota''(0)$	Q
0.16	1.0749×10^{-2}	0.1181	1.0749×10^{-2}	0.1179
0.14	6.8338×10^{-3}	0.1058	6.8338×10^{-3}	0.1055
0.12	3.9346×10^{-3}	0.0961	3.9346×10^{-3}	0.0959
0.10	1.9356×10^{-3}	0.0896	1.9356×10^{-3}	0.0893
0.09	1.2382×10^{-3}	0.0878	1.2382×10^{-3}	0.0875
0.08	7.2152×10^{-4}	0.0871	7.2152×10^{-4}	0.0868
0.07	3.6698×10^{-4}	0.0879	3.6700×10^{-4}	0.0875
0.0237			10^{-8}	0.1060
0.0207			10^{-9}	0.1069
0.0184			10^{-10}	0.1075
0.0151			10^{-12}	0.1082
0.0128			10^{-14}	0.1085
0.0111			10^{-16}	0.1086
0.0098			10^{-18}	0.1085

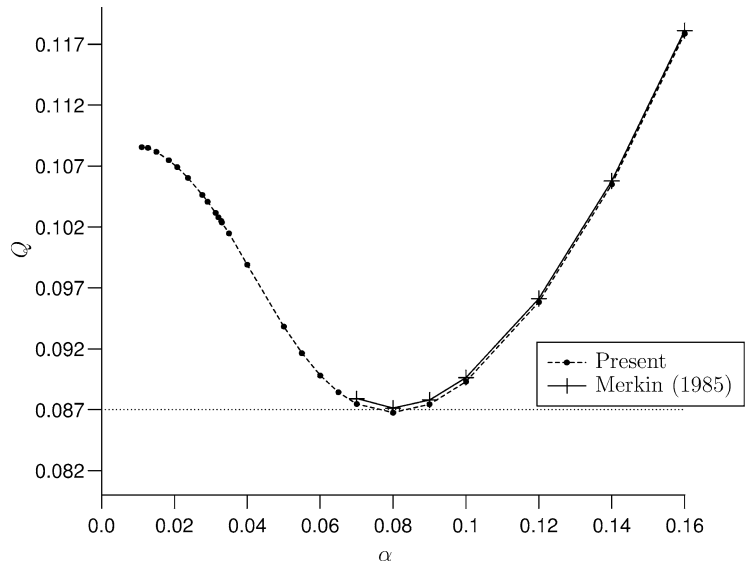

Fig. 9. Variation of Q as a function of α for data as given by Merkin [11], with $a_0 = 0.8758$, and the present work, with $a_0 = 0.8754$.

to 0.083. On using the same technique as Merkin [11], we observe a value of $A_1 \approx 0.1085$. However, in the present work we obtained a more accurate value of A_1 from the values of $f_\iota''(0)$ that are very close to $\alpha = 0^+$ by another technique. This involves taking the ln of Eq. (25) to produce

$$\ln\bigl(f_\iota''(0)\bigr) = \ln(A_1) - \frac{a_0^2}{2}\alpha^{-1}. \tag{27}$$

On applying a least squares fit to the values of $\ln(f_\iota''(0))$ as a function of (α^{-1}), we found that Merkin's [11] values did not produce an exact linear variation, i.e., a regression coefficient $r^2 = 0.9978$, while for the present data the variation is, to within the numerical accuracy, exactly linear, i.e., $r^2 = 1$, even if additional values of α are included, and therefore the values of a_0 and A_1 in the present work, namely $a_0 = 0.8754$ and $A_1 = 0.1085671$, are an improvement compared with the values given by Chapman [17] and Merkin [11], respectively.

From Fig. 9, we observe that the curves decrease rapidly as α decreases until a minimum is obtained near $(0.08, 0.087)$, before the curves begin to rise rapidly.

Furthermore, we observe that the two curves are almost identical for large values of α and they have their greatest difference for values of α below $\alpha = 0.08$. This suggests that the value A_1, as obtained from the present work, is more accurate than that obtained by Merkin [11]. The above discussion suggests that using a variation of A_1 as a function of α as $\alpha \to 0^+$ may enable $f_\iota''(0)$ to be calculated more accurately from Eq. (25) and with $a_0 = 0.8754$, we assume the relation

$$A_1 = a_1 + a_2\alpha + a_3\alpha^2 + \cdots, \tag{28}$$

where a_1, a_2 and a_3 are constants to be determined. On using Maple, programme version 6, we found that $a_1 = 0.1047$, $a_2 = 0.002$ and $a_3 = -0.0103$.

For $\lambda < 0$, the variation of $f''(0)$ with ε terminates at $\varepsilon = -1$ and the following theory validates this. We again look for the solution of the full equations near $\varepsilon = -1$ for $\lambda < 0$. On solving Eq. (23), subject to the boundary condition (22), for $\lambda < 0$, we obtain

$$f_\iota(\eta) = \frac{(1+\varepsilon)}{\sqrt{-2\lambda}}\sinh(\sqrt{-2\lambda}\,\eta) + \frac{f_\iota''(0)}{2\lambda}\big[1 - \cosh(\sqrt{-2\lambda}\,\eta)\big]. \tag{29}$$

To investigate if expression (29) can be taken to represent the inner solution for $\lambda < 0$, we have studied the vertical component of the velocity for $\lambda = -0.02$ where $\varepsilon = -1.2, -1.15$ and -1.1, and also for $\lambda = -0.1$, where $\varepsilon = -1.25, -1.223$ and -1.2222, corresponding to the lower solution in the range $0 \leqslant \eta \leqslant 5$ for the full equation (14) and expression (29), on using the value of $f''(0)$ obtained from the numerical solution, respectively. As the two curves are almost identical in the range $0 \leqslant \eta \lesssim 1.5$, expression (29) may be taken to represent the inner solution for $\lambda = -0.02$ and $\lambda = -0.1$, and hence for $\lambda < 0$.

5. Solution for $0 < \varepsilon \ll 1$

We now look for a solution of Eqs. (10) and (11), subject to the boundary conditions (12) and (13), which is valid for values of ε close to zero in the following form:

$$f(\eta) = \sum_{i=0}^{\infty} \varepsilon^i f_i(\eta), \qquad \theta(\eta) = \sum_{i=0}^{\infty} \varepsilon^i \theta_i(\eta). \tag{30a,b}$$

On substituting these expressions into Eqs. (10) and (11) and into the boundary conditions (12) and (13) and equating powers of ε, we obtain the following:

(i) The ε^0 solution is given by

$$\theta_0(\eta) = 2^s\Gamma\left(\frac{s}{2}+1\right)\mathrm{i}^s\,\mathrm{erfc}\left(\frac{\eta}{\sqrt{2-s}}\right), \tag{31}$$

where s is a constant defined by $s = 2\lambda/(1+\lambda)$, Γ is the gamma function and erfc is the complementary error function, see Abramowitz and Stegun [18]. However, the only possible values are $s = -1, 0$ and 1, where $\lambda = -\frac{1}{3}, 0$ and 1, respectively. We have numerically solved the full equations and from Eq. (33), we obtain $f_1''(0) = 0, -0.7979$ and -1.7725 for $\lambda = -\frac{1}{3}, 0$ and 1, respectively. As expected, these values are identical to those obtained from the first term of the asymptotic expansion in expression (30b), when substituting $\eta = 0$ in the differentiation of Eq. (31).

If $\lambda > -1$, and $\lambda \neq -\frac{1}{3}, 0$ or 1, then we have found that the general solution is given by

$$\theta_0(\eta) = (1+\lambda)2^{-(5\lambda+1)/(4(\lambda+1))}\eta^{-1/2}\,\mathrm{e}^{-((1+\lambda)/4)\eta^2}W_{(-(5\lambda+1)/(4(\lambda+1)),-1/4)}\left(\frac{1+\lambda}{2}\eta^2\right), \tag{32}$$

where W is the Whittaker function, see Whittaker and Watson [19].

(ii) The ε^j solution ($j > 0$) is

$$f_j' = \theta_{j-1}, \tag{33}$$

$$\theta_j'' + (1+\lambda)\sum_{i=0}^{j} f_i\theta_{j-i}' - 2\lambda\sum_{i=0}^{j} f_i'\theta_{j-i} = 0, \tag{34}$$

which have to be solved subject to the boundary conditions:

$$f_j(0) = 0, \qquad \theta_j(0) = 0, \tag{35}$$

$$f_j' \to 0, \quad \theta_j \to 0, \quad \text{as } \eta \to \infty. \tag{36}$$

We require to find $f''(0)$ and it is given by

$$f''(0) = \sum_{i=1}^{\infty} \varepsilon^i f_i''(0) = \sum_{i=1}^{\infty} \varepsilon^i \theta_{i-1}'(0). \tag{37}$$

We have studied the variation of $f''(0)$ as a function of ε for $-1.4 \leqslant \varepsilon \leqslant 2$ when $\lambda = -0.1$, 0 and 0.1, respectively, for the full numerical solution of Eq. (14) and for 1, 2, 3, 5 and 10 terms of the expansion (30a). As we would expect, we found that increasing the number of terms in the expansion (30a) increases the range of values of ε for which the series solution (30a) gives accurate values of $f''(0)$. Finally, we have studied the numerically obtained values of $f_i''(0) = \theta_{i-1}'(0),\ i = 1, 2, \ldots, 9, 10$ for $\lambda = -0.1$, 0 and 0.1. We found that the values of $|f_i''(0)|$ decrease as i increases and for i large then the ratio $|f_{i+1}''(0)/f_{i+2}''(0)|$ is about 0.5 and this is the reason why reasonably accurate results may be obtained for $f''(0)$ and $\theta'(0)$ up to values of $\varepsilon \approx 2$.

6. Asymptotic solution ($\varepsilon \gg 1$)

Fig. 3(b) shows the variation of $f''(0)$ as a function of ε for $\lambda = 0.05$ and $-1.364 \leqslant \varepsilon \leqslant 100$. We observe that the two solutions, $f_u''(0)$ and $f_l''(0)$, are very similar for large values of ε. We now seek a new set of full equations which do not contain ε on using the following transformation

$$f(\eta) = \eta + \varepsilon^{\vartheta} H(\zeta) \quad \text{where } \zeta = \varepsilon^{\gamma} \eta, \tag{38}$$

where ϑ and γ are constants to be determined. On substituting expressions (38) into Eq. (14), we obtain

$$\varepsilon^{2\gamma} H''' + (1+\lambda)\varepsilon^{\gamma} \eta H'' + \varepsilon^{\vartheta+\gamma}\left[(1+\lambda) H H'' - 2\lambda H'^2\right] - 2\lambda H' = 0. \tag{39}$$

In order to ensure that the highest derivative remains present in the resulting equation, so avoiding the need to disregard any of the boundary conditions, we look for a balance within the equation of this term, see Holmes [20]. Hence we obtain $\vartheta = \gamma = \frac{1}{2}$. Therefore, when $\varepsilon \to \infty$ we obtain the following new set of full equations

$$H''' + (1+\lambda) H H'' - 2\lambda H'^2 = 0, \tag{40}$$

$$H(0) = 0, \qquad H'(0) = 1, \qquad H' \to 0, \quad \text{as } \zeta \to \infty. \tag{41}$$

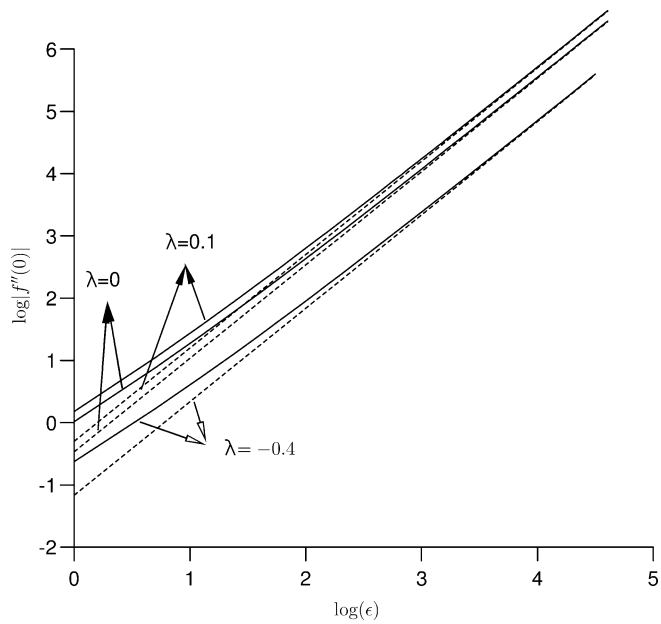

Fig. 10. The variation of $\log(|f''(0)|)$ as a function of $\log(\varepsilon)$. The dashed line is the solution of Eq. (40), subject to the boundary conditions (41), for $\lambda = 0,\ \lambda = 0.1$ and $\lambda = -0.4$, while the solid line is the solution of Eq. (14), subject to the boundary conditions (15), for $\lambda = 0,\ \lambda = 0.1$ and $\lambda = -0.4$.

Furthermore, the relation between $f''(0)$ and $H''(0)$ is given by

$$f''(0) = \varepsilon^{3/2} H''(0). \tag{42}$$

The boundary conditions (41) do not contain ε and thus, on solving Eq. (40) subject to these conditions, we obtain a value of $H''(0)$ which is independent of ε. Then on using the relation (42), we obtain the value of $f''(0)$ for any value of $\varepsilon \gg 1$.

From Fig. 10, we observe that the accuracy of the two solutions increases as $\log(\varepsilon)$ increases until the two curves are graphically almost indistinguishable for large values of ε, say $\varepsilon > 100$. So for large $|\varepsilon|$ we can replace the solution of the full equations with the solution of Eq. (40), subject to the boundary conditions (41), which are independent of ε.

7. Conclusions

In this paper we have investigated the problem of a thin vertical fin, which is modelled as a fixed, semi-infinite vertical surface which is embedded in a fluid-saturated porous media which is maintained at a constant temperature, and in which a vertical free stream is flowing. For the numerous situations we have considered, we made the following conclusions:

(i) For $\lambda = 0$ and $\varepsilon < 0$, we have obtained numerical solutions very close to the point where the numerical solution appears to terminate, i.e., near $\varepsilon = -1$. Thus we have been able to discuss in more detail than Merkin [16] was able to, the velocity profiles and the shear stress. In particular, Merkin [16,11] found numerically that as $\varepsilon \to -1^-$ then $f_l''(0) \to 0$ and, in the inner region $f_l \simeq (1+\varepsilon)\eta$, but we have found this result analytically, using his assumptions.

(ii) For $\lambda > 0$, we have found that, for a given value of λ, there are, over a range of values of ε, two solutions. We have studied the variation of $f''(0)$ as a function of ε, the velocity profiles and the shear stress for $-1.3640 \leqslant \varepsilon < \infty$ for $\lambda = 0.05$. For other values of λ, we have found that results obtained show a very similar behaviour as for $\lambda = 0.05$. In this case the numerical solution does not terminate.

(iii) For $\lambda < 0$, we have found that, for a given value of λ, there are two solutions which are very different from those obtained for $\lambda > 0$. Unfortunately, the solution appears to terminate at a value of ε and we were numerically unable to continue the lower solution after this value of ε. On investigating the possible existence of a universal curve, we have found that the results suggest the possibility of a universal curve which is independent of λ. Finally, we have solved analytically the full equations near $\varepsilon = -1$ and we have concluded that this solution may be taken to represent the inner solution.

(iv) For $0 < \varepsilon \ll 1$, we have found the solution for the order ε^0, which is restricted to some certain values of λ. Furthermore, we have compared the value of $\theta_0'(0)$ as obtained from the numerical solution and the analytical solution at these values of λ and we have found that they are virtually indistinguishable. In addition, we have obtained the general expression for θ_0. For the order ε^j $(j > 0)$ terms, we have compared the results obtained for the full numerical solution with the results obtained using various number of terms in the series solution expansion and we have found, as expected, that increasing the number of terms in the expansion increases the range of values of ε for which the series solution gives accurate predictions of $f''(0)$.

(v) For $\varepsilon \gg 1$, we have introduced a new governing equation and boundary conditions which do not contain ε in the limit as $\varepsilon \to \infty$. On comparing the values of $\log|f''(0)|$ as a function of $\log(\varepsilon)$ as obtained from the solution of the full equations and the new equation, we have found, as expected, that the accuracy of the two solutions increases as $\log(\varepsilon)$ increases until the two curves are graphically almost indistinguishable for large values of ε. Therefore for large $|\varepsilon|$ we can replace the solution of the full equations by the new equation which are independent of ε.

Finally, although we have taken a very idealised model of a fin, the results obtained in this investigation indicate some of the issues that must be addressed when investigating fins of more realistic orientation and thickness. The main practical points to note are as follows:

(a) For aiding flows, i.e., $\varepsilon > 0$. If $\lambda > 0$, then there are two solutions and the upper solution is likely to be the physical and stable solution. However, if $\lambda < 0$ there is only one solution.

(b) For opposing flows, i.e., $\varepsilon < 0$. As expected, if the opposing flow is too large then the boundary-layer theory will break down and we will obtain no solution. In this case we have to solve the full elliptic equation. However, there will be a range of small negative values for which it may be possible to obtain either two solutions ($\lambda \gtrless 0$) or no solution for a range of values of ε and two solutions in another range of values of ε ($\lambda \gtrless 0$).

(c) The asymptotic analytical solutions presented in Sections 5 and 6 can be used for predecting the Nusselt number.

In summary, the governing equations and boundary conditions that we have derived for this fin problem are more general than those considered by other authors and therefore our analysis is applicable to a large range of physical situations.

Acknowledgements

The authors would like to thank the referees for their careful reading of the original manuscript and their constructive comments.

One of the authors (E.H.A.) gratefully thanks the partial financial support of the King Faisal Foundation, Saudia Arabia and of the University of Leeds. Another author (D.B.I.) would like to thank the Royal Society for some financial support for this work.

References

[1] D.B. Ingham, I. Pop, Transport Phenomena in Porous Media, Pergamon, Oxford, 1998.
[2] D.A. Nield, A. Bejan, Convection in Porous Media, 2nd edition, Springer, New York, 1999.
[3] I. Pop, D.B. Ingham, Convection Heat Transfer, Mathematical and Computational Modelling of Viscous Fluids and Porous Media, Pergamon, Oxford, 2001.
[4] E.M. Sparrow, R. Eichhorn, J.L. Gregg, Combined forced and free convection in boundary layer flow, Phys. Fluids 2 (1959) 319–328.
[5] P. Cheng, Combined free and forced convection flow about inclined surfaces in porous media, Int. J. Heat Mass Transfer 20 (1977) 807–814.
[6] J.H. Merkin, The effect of buoyancy forces on the boundary-layer over a semi-infinite vertical flat plate in a uniform free stream, J. Fluid Mech. 35 (1969) 439–450.
[7] G. Wilks, Combined forced and free convection flow on vertical surfaces, Int. J. Heat Mass Transfer 16 (1973) 1958–1963.
[8] G. Wilks, A separated flow in mixed convection, J. Fluid Mech. 62 (1974) 359–368.
[9] R. Hunt, G. Wilks, On the behaviour of the laminar boundary-layer equations of mixed convection near a point of zero skin friction, J. Fluid Mech. 101 (1980) 377–391.
[10] G. Wilks, S.J. Bramley, Dual solutions in mixed convection, Proc. Roy. Soc. Edinburgh Sect. A 87 (1981) 349–358.
[11] J.H. Merkin, On dual solutions occurring in mixed convection in a porous medium, J. Engrg. Math. 20 (1985) 171–179.
[12] J.H. Merkin, T. Mahmood, Mixed convection boundary layer similarity solutions: prescribed wall heat flux, J. Appl. Math. Phys. (ZAMP) 40 (1989) 51–68.
[13] A. Ridha, Aiding flows non-unique similarity solutions of mixed convection boundary-layer equations, J. Appl. Math. Phys. (ZAMP) 47 (1996) 341–352.
[14] J.H. Merkin, I. Pop, Mixed convection along a vertical surface: similarity solutions for uniform flow, Fluid Dyn. Res. 30 (2002) 233–250.
[15] P. Cheng, W.J. Minkowycz, Free convection about a vertical flat plate embedded in a porous medium with application to heat transfer from a dike, J. Geophys. Res. 82 (1977) 2040–2044.
[16] J.H. Merkin, Mixed convection boundary layer flow on a vertical surface in a saturated porous medium, J. Engrg. Math. 14 (1980) 301–313.
[17] D.R. Chapman, Laminar mixing of a compressible fluid, NACA Rep. 958, 1950.
[18] M. Abramowitz, I.A. Stegun, Handbook of Mathematical Functions, 4th edition, Dover, New York, 1972.
[19] E.T. Whittaker, G.N. Watson, A Course of Modern Analysis, 4th edition, 1962, Cambridge.
[20] M.H. Holmes, Introduction to Perturbation Methods, in: Texts in Appl. Math., Vol. 20, Springer, New York, 1995.